X-ray Spatial and Energy Response of a 3-D Silicon Detector

J. Morse,[1] C.J. Kenney,[1] E.M. Westbrook,[1] I. Naday,[2] S.I. Parker[3]
[1]Molecular Biology Consortium, Chicago, IL, U.S.A.
[2]Argonne National Laboratory, Argonne, IL, U.S.A.
[3]University of Hawaii, Manoa, HI, U.S.A.

Introduction

"3-D" silicon detectors have been fabricated with alternate arrays of n- and p-type column electrodes perpendicular to the detector's surface, penetrating entirely through the silicon wafer. This geometry can be contrasted with that of a conventional planar detector, in which the electrode structures are parallel to the surface of the detector material and limited by processing technology to depths within a few microns of the wafer surfaces. We are building a large pixel detector for macromolecular crystallography that will consist of several hundred 3-D detectors, tiled in an array to cover an area of ~200 × 200 mm^2 [1]. Planar silicon detectors need a guard ring structure at their cut edges to control local electric field strength and thus avoid large surface leakage currents. For a tiled array detector, the active area lost to adjacent peripheral guard rings creates an X-Y grid of dead bands with a width of ~500 μm, typically wasting 5% to 10% of the total detector surface [2, 3]. In contrast, our 3-D architecture has no vertical electric field component at the cut edges. By using vertical plasma etching, it is possible to process the detectors so that they are sensitive to within <10 μm of their physical edges, which can be made as conductive boundary electrodes. The concept, simulation [4], and fabrication [5] of silicon 3-D detectors and the architecture of the devices investigated here were reported previously on [6]. Presented here are new measurements that were made with an x-ray beam with a cross section of <10 μm, which enabled us to study the detailed spatial-energy response of the detectors for the first time.

Methods and Materials

3-D detectors with a matrix of 12 × 17 pixels covering an area of 1.2 × 3.2 mm^2 were fabricated from 121-μm-thick silicon. They have 12 sets of p-type column electrodes electrically connected by aluminium contact strips deposited on the detector surface to form parallel line segments. Each column electrode extends completely through the silicon wafer and consists of a doped, polycrystalline silicon core from which dopant atoms have been diffused into the surrounding single-crystal silicon. The physical diameter of the polycrystalline silicon cores, as measured by optical microscopy, was 23 μm. Figure 1 is a schematic representation of a fragment of the detector.

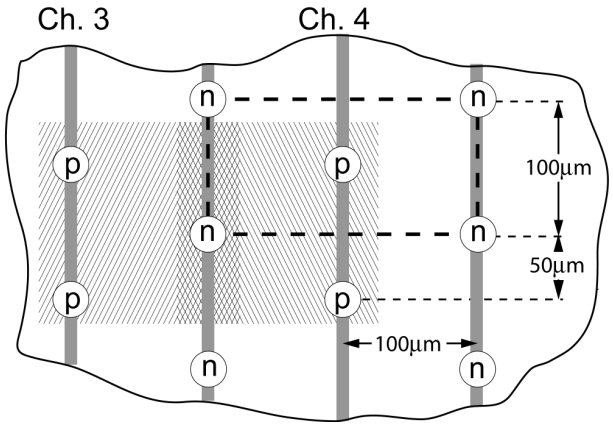

FIG. 1. Schematic of the 3-D detector tested. A pixel cell consists of a p electrode surrounded by four 1/4 n electrodes. The grey vertical stripes represent aluminium surface traces that connected the column electrodes. The overlapping, hatched rectangles correspond to the areas of the detector that were scanned.

The detector tested was depleted at 5 V and operated at 20 V with a total bias leakage current of 7 μA (23°C). This large bias current was attributed to peripheral surface currents, since good x-ray spectra would have been impossible to measure if significant currents (> nanoampere-sized) had been flowing to the sensing column electrodes themselves. Previous probe measurements made on 3-D detectors taken from the same production batch showed intercolumn electrode leakage current densities of only 0.6 to 1.3 nA mm^{-3}. Each of the p-type electrode contact strips was directly wire-bonded to a charge-sensitive preamplifier channel of an adjacent application-specific integrated circuit (ASIC) chip, which included a CR-RC shaping filter with rise/fall times of approximately 0.6/2 μs. All x-ray data were acquired at low count rates (<7 kilo counts per second or kcps) to ensure negligible degradation from pulse pile-up artifacts. The x-ray beam energy chosen to characterize the 3-D detector was 12.65 keV, corresponding to selenium replacement in the MAD technique used in macromolecular diffraction experiments.

The spatial profile of the x-ray beamline at station 13-BM-D at the APS was measured by a knife edge

scan with a scintillation counter after the beam had passed through crossed, tapered-cylinder microslits. This gave the beam full widths of 8 and 12 μm in the X and Y directions, respectively, at the position of the 3-D detector. The 3-D detector was then mounted and raster-scanned through this beam over 16×16 points at 10-μm step intervals. Energy histogram data were accumulated at each raster point for the two horizontally adjacent pixels corresponding to detector readout channels 3 and 4. As shown in Fig. 1, the overlapping scans of channels 3 and 4 covered the critical interpixel boundaries where charge sharing must occur.

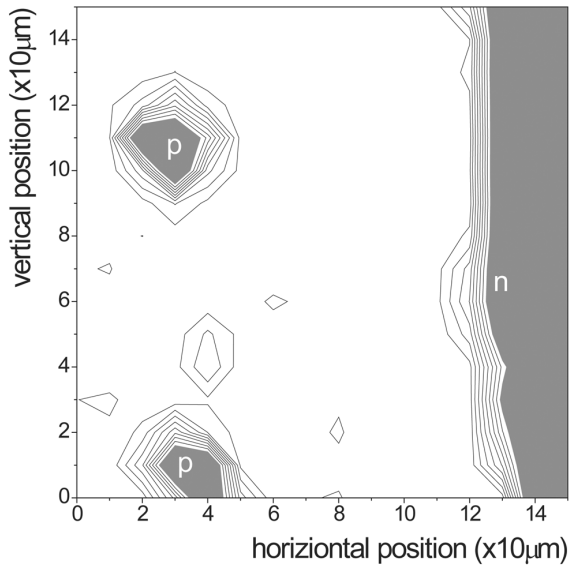

FIG. 2. Response of channel 4 to a vertical-horizontal raster scan at 10 μm step intervals. The contour lines are at 3% intervals of the nominal response of 3.4×10^4 counts per scan point (5-second integration). Grey-filled areas showed <73% of the nominal response.

Results

Figure 2 shows the response of part of a pixel corresponding to readout channel 3. To generate this contour map, integral counts were evaluated for the 256 individual energy histograms of the raster scan with a lower-level energy threshold set at 10 keV that was applied in the software.

Setting the energy threshold at this high level makes the contour map sensitive to any loss in energy for individual events (e.g., as a result of incomplete charge collection). The positions of two vertically adjacent p-column electrodes are clearly defined, as is the fall-off in response at the limit of the vertical pixel boundary to the right and as is the outline of the n-column electrode that is shared at the pixel boundary. Within the surface areas covered by the electrodes, very little x-ray

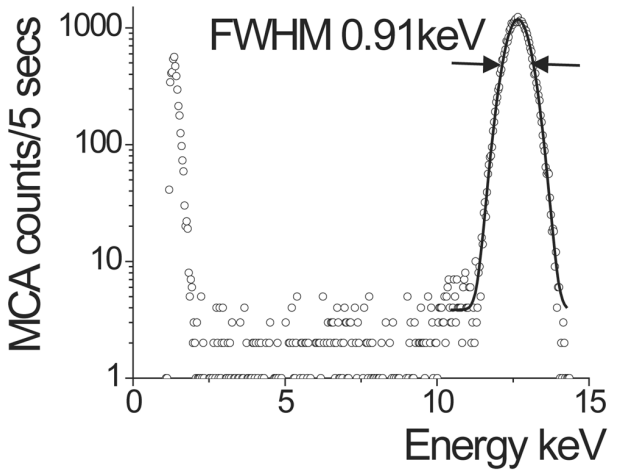

FIG. 3. Channel 3 energy spectrum measured with beam inside pixel boundary (beam at X,Y position 90, 0 μm in Fig. 2).

response is seen. This is expected as a result of the estimated charge carrier lifetime of only nanoseconds within the polycrystalline silicon that forms these electrodes and the lack of any charge-separating drift field within them. The effective diameter of the electrodes is not precisely defined because of the relatively coarse 10 μm sampling interval of the measurement. Figure 3 shows the excellent energy response of the detector, with the photopeak well-fitted by a simple Gaussian profile of width 0.91 keV full height at half-maximum (FHHM). This photopeak energy width is dominated by the ASIC preamplifier electronic noise. The absence of any tailing of the peak toward low energies is a stringent test confirming complete charge collection.

The 3-D representation of Fig. 4 is a composite map of the response of two adjacent pixels corresponding to readout channels 3 (left) and 4 (right). To create this, energy histogram data were summed with a lower-level threshold reduced to 6 keV (i.e., about half the photopeak energy). The "counts above threshold" response within the pixel is uniform at the level of statistical precision to ~1%, except at the column electrodes and at the vertical boundary between the pixels of channel 3 and 4. This measurement was the first direct confirmation that the fall-off in response is localized at these features, at least on the scale of ~10 μm (i.e., the measurement precision imposed by the probing x-ray beam size and step interval).

There is a vertical strip (at horizontal position ~150 mm) in which the count response reaches up to ~60% higher than the surrounding plateau. This is the result of double-counting single x-rays at the vertical pixel boundary. The fraction of double-counted events depends strongly on the setting of the "counting"

energy threshold. Figure 5a is a horizontal section through the 3-D plot of Fig. 4 evaluated at the vertical position of 120 μm, corresponding to a line that passes through the p electrode centers. The large double-count excess at the energy threshold of 6 keV drops, becoming deficit as the threshold used in the analysis is increased to 9 keV. Figure 5b shows the response of a horizontal line section through a nearest neighbor set of p electrodes, with a much reduced double-count or lost count effect. This apparently conflicting result is believed to result from the 3-D detector having been mounted with a skew about the beam axis. A vertical angle error of 3° would have resulted in a 5-μm offset between the spatial samplings of the data shown in Fig. 5, a and b, while the spatial extent over which charge splitting at the pixel boundary occurs is apparently ~10 μm (refer to Fig. 2). The spatial sampling interval of 10 μm is too low to accurately represent data from features of this width. There is no evidence of a change in count rate as the x-ray beam was scanned vertically across the horizontal boundary between adjacent pixels. As the p electrodes of these pixels were electrically "shorted" together in the vertical direction by their aluminium surface connections, the signal charge contributions from these pixels were analog-summed at the preamplifier input before the resultant total signals were compared with the 6-keV energy threshold that was applied in the software. Therefore, for the vertically adjacent pixels, the threshold effect on the perceived count rate due to charge splitting is completely eliminated if all charge carriers are collected from either side of the geometrical pixel boundary.

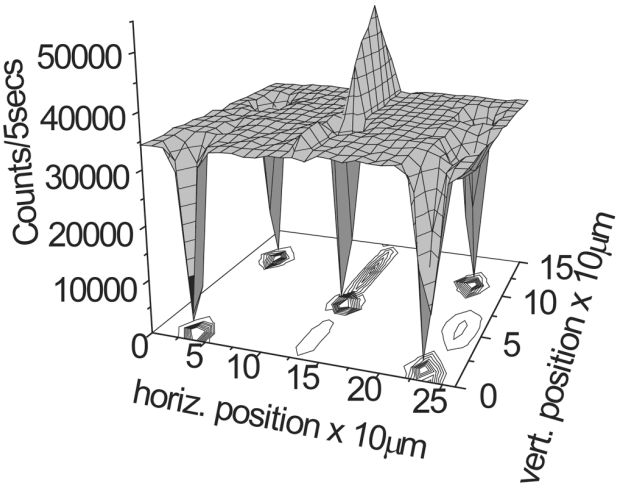

FIG. 4. Composite map from integral counts above an energy threshold of 6 keV, from successive measurements on channels 3 and 4.

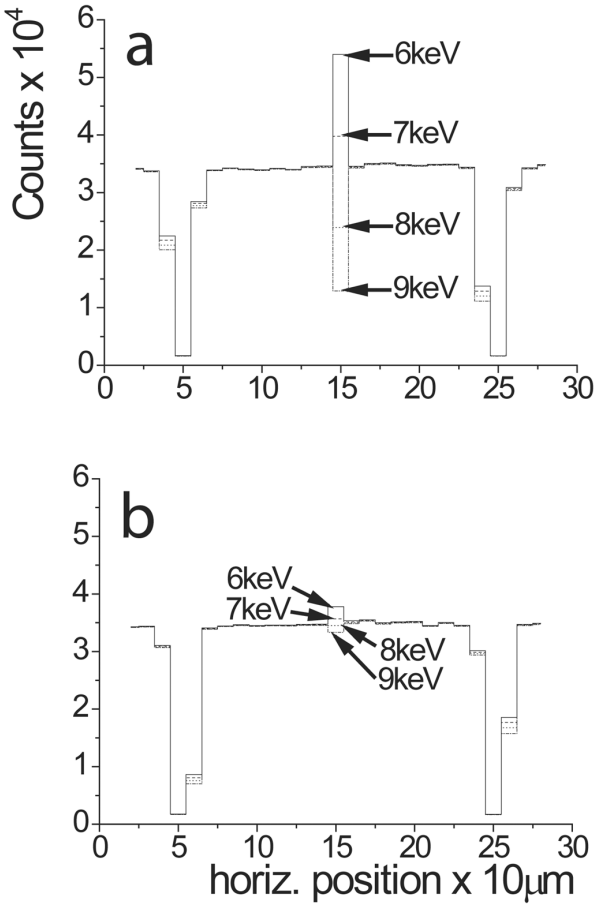

Figs 5a, b: Horizontal line sections through the surface of Fig. 4, passing through the p-electrode centers at vertical positions 120μm (a) and 20μm (b). Integral 'count' responses are shown, corresponding to threshold energies at 6, 7, 8 and 9keV.

Discussion

We have demonstrated that 3-D detectors can show excellent charge collection resulting in tail-free energy spectra. No x-ray response is seen at the polycrystalline electrodes of these detectors, but these dead areas are shown not to extend beyond the diameters of the electrodes themselves. Charge splitting between adjacent pixels is confined within a band that is certainly <20-μm wide, and a uniform response was measured across a horizontal pixel boundary where the split charge was analog-summed, implying no loss of signal charge. For a practical detector, the need to implement analog charge summation at pixel boundaries is made evident by the strong modulation in count rate that is observed at a vertical pixel boundary when a simple threshold, integral counter approach is used to analyse the data.

Acknowledgments

We are especially grateful to M. Rivers and M. Newville of the GSECARS CAT for their essential support during the beamline station 13-BM-D tests. Use of the APS was supported by the U.S. Department of Energy, Office of Science, Office of Basic Energy Sciences, under Contract No. W-31-109-ENG-38. The processing of the 3-D silicon detectors was carried out at the Nanofabrication Facility of the Center for Integrated Systems at Stanford University, which is supported by the National Science Foundation. Development of 3-D detectors for protein crystallography applications is administered by the Molecular Biology Consortium under a National Institutes of Health, National Center for Research Resources Grant No. 1 R01 RR1 6230-01. This work has been submitted for publication to *Nuclear Instruments and Methods*.

References

[1] J. Morse, C. Kenney, E. Westbrook, I. Naday, and S. Parker, Proc. SPIE-Int. Soc. Opt. Eng. 4784, 365-374 (2002).

[2] G. Iles, K. Mathieson, P. Murray, S. Passmore, M. Prydderch, P. Seller, and S. Thomas, Nucl. Instrum. Methods A 458(1-2), 427-430 (2001).

[3] C. Brönniman, R. Baur, E. Eikenberry, P. Fischer, S. Florin, R. Horisberger, M. Lindner, B. Schmitt, and C. Schulze, Nucl. Instrum. Methods A 477, 531-535 (2002).

[4] S. Parker, C. Kenney, J. Segal, Nucl. Instrum. Methods A 395, 328-343 (1997).

[5] C. Kenney, S. Parker, J. Segal, and C. Storment, IEEE Trans. Nucl. Sci. 46(4), 1224-1236 (August 1999).

[6] C. Kenney, S. Parker, B. Krieger, B. Ludewigt, T. Dubbs, and H. Sadrozinski, IEEE Trans. Nucl. Sci. 48(2), 189-193 (April 2001).